Effects of Jatropha oil blending with C-heavy oil on soot emissions and heat absorption balance characteristics for boiler combustion

Nozomu HASHIMOTO[1,2], Hiroyuki NISHIDA[1], Msayoshi KIMOTO[1], Kazuki TAINAKA[1], Atsushi IKEDA[1], Satoshi UMEMOTO[1]

1. Central Research Institute of Electric Power Industry (CRIEPI), 2-6-1 Nagasaka, Yokosuka, 240-0196 Japan
2. Hokkaido University, Kita 13 Nishi 8, Kita-ku, Sapporo, 060-8628, Japan

Correspondence: Nozomu HASHIMOTO
Division of Mechanical and Space Engineering, Graduate School of Engineering, Hokkaido University, Kita 13 Nishi 8, Kita-ku, Sapporo, 060-8628, Japan
Phone: +81-11-706-6386
FAX: +81-11-706-6386
E-mail: nozomu.hashimoto@eng.hokudai.ac.jp

Declarations of interest: none

Abstract

This study investigated the effect of crude *Jatropha* oil (CJO) blending with C-heavy oil on the combustion characteristics of oil-fired boilers. Combustion experiments were conducted using a 550 kW liquid fuel combustion test facility equipped with a steam-atomizing burner. The results indicated that the flame radiation intensity is decreased by the CJO blending with C-heavy oil. Consequently, the heat absorption of the sections near the burner decreases. Due to the lower nitrogen and sulfur contents in CJO, the NOx and SO_2 emissions are decreased by the CJO blending with C-heavy oil. It was also found that both the particulate matter concentration and the particle size in the exhaust gas are decreased by the CJO blending. This is attributed by the low carbon residue content of CJO. The results of this study imply that when CJO is introduced into oil-fired thermal power stations, considerable attention should be paid to changes in the heat absorption balance and the possibility of a decrease in the particle collection efficiency of the electrostatic precipitator.

Key words: spray combustion; *Jatropha* oil; heavy oil; soot formation; heat absorption balance

Nomenclature

C_1: first Planck's constant, 3.742×10^{-16} Wm^2

C_2: second Planck's constant, 1.439×10^{-2} mK

$c_{p,water}$: specific heat of water, J/(kg K)

E: flame radiation intensity, W/m^2

$E_{\lambda i}$: monochromatic radiation intensity for λ_i, W/m^3

K: absorption coefficient, 1/m

L: line-of-sight path length through flame, m

$\dot{m}_{water,i}$: mass flow rate of cooling water supplied to section i, kg/s

$\dot{Q}_i$: heat absorption rate of section i, W

T: temperature of soot particles in the flame, K

T_{in}: temperature of cooling water supplied to each section, K

$T_{out,i}$: temperature of cooling water discharged from section i, K

$X_{4\%O2,i}$: volumetric concentration of species i corrected to 4% O_2, ppm

$X_{measured,i}$: volumetric concentration of species i measured in exhaust gas, ppm

$X_{m,O2}$: volumetric concentration of O_2 measured in exhaust gas, %

Greek Symbols

α: constant

$\varepsilon_{\lambda i}$: monochromatic emissivity for λ_i

λ_i: wavelength, m

1. Introduction

Biomass fuel attracts considerable attention as a renewable energy source from the viewpoint of global warming. Vegetable oil can be used as an alternative biomass-derived fuel in oil-fired thermal power stations. The vegetable oil from *Jatropha curcas* is a promising biomass-derived fuel as it does not directly influence food prices because of its toxicity. Another advantage of *Jatropha* is the wider latitude range in which it can be cultivated compared with that of palm [1]. In addition, *Jatropha* is a drought-resistant perennial plant that grows well even in marginal soil [1]. According to a report by the Global Exchange for Social Investment (GEXSI) [2], there are considerable areas of land where *Jatropha* can be cultivated, whereas other edible crops cannot be cultivated. Although the oil yield of palm trees exceeds that of *Jatropha* [3], a report indicated that the net energy ratio (ratio of energy output to energy input) of *Jatropha* oil was higher than that of palm oil when considering the energy content of the co-products [4]. Therefore, the fundamental combustion characteristics have been investigated using basic burners by some researchers [5,6].

As *Jatropha* oil can be utilized as an alternative fuel for automobiles, stationary gas turbines, and airplanes, previous researches have investigated its combustion characteristics for IC engines [7-24] and gas turbine combustors [25-31]. However, IC engines and gas turbine combustors require the purification and/or esterification of *Jatropha* crude oil to eliminate impurities and/or to decrease the viscosity to achieve acceptable atomization characteristics. In contrast, purification and esterification are not required for boilers as they have higher tolerance for impurities and the viscosity of the fuel compared with IC engines and gas turbine combustors. However, there are very few studies

investigating the combustion characteristics of *Jatropha* oil for boilers. A study by Kang et al. [32] is one of the few studies in which direct burning of crude *Jatropha* oil (CJO) in a commercial boiler system using a burner designed for commercial home-heating oil was conducted. The study revealed that CO, NOx and soot emissions from CJO combustion were comparable to the emissions from the commercial home-heating oil. However, it is necessary to investigate the combustion characteristics of CJO using a burner designed for C-heavy oil in order to introduce CJO into oil-fired thermal power stations. Since the spray combustion is a complicated phenomenon, the various fundamental researches have been conducted by many researchers [33-38]. Such fundamental researches are important to clarify the basic mechanism of the spray combustion. On the other hand, the evaluation whether there will be problems or not when a new type of fuel is introduced.

The aim of this study is to evaluate the effect of CJO blending with C-heavy oil in oil-fired thermal power stations. A 550 kW liquid fuel combustion test facility equipped with a burner designed for C-heavy oil [39] was used for the evaluation. Two combustion tests involving pure C-heavy oil and a mixed fuel of 50% CJO and 50% C-heavy oil on a lower heating value (LHV) basis were conducted. The NOx, SO_2 and particulate matter emissions were compared for the two cases. Furthermore, the two cases were also compared with respect to the particle size distributions in the exhaust gas, the flame radiation intensities, and the heat absorption balances. Although the number of combustion tests were limited owing to a large consumption rate of fuel, unique experimental data, which are beneficial for examinations of introducing biofuels into oil-fired thermal power stations, were obtained.

40

41 **2 Experimental apparatus and conditions**

42 **2.1 Fuel properties**

43 The properties of the fuels investigated in this study are listed in Table 1. The density and LHV
44 of CJO are lower than that of C-heavy oil. This indicates that the volumetric flow rate of CJO
45 exceeds that of C-heavy oil for the same thermal input to the boiler. The viscosity of CJO is much
46 lower than that of C-heavy oil. The temperature of CJO needed to achieve the required atomization

Table 1 Fuel Properties.

Item \ Fuel			C-heavy oil	CJO
Density	@30℃	g/cm^3	0.9635	0.9097
	@50℃	g/cm^3	0.9492	0.8962
	@75℃	g/cm^3	0.9317	0.8793
Kinematic viscosity	@30℃	mm^2/s	392.0	52.6
	@50℃	mm^2/s	110.0	25.8
	@75℃	mm^2/s	36.8	13.1
Surface tension	@23℃	dyn/cm	30.6	31.7
	@50℃	dyn/cm	29.2	29.6
HHV		J/g	42,820	39,670
LHV		J/g	40,450	37,026
Flash point		℃	93	248
Ignition point		℃	408	417
Water content		wt-ppm	300	1,100
Ultimate analysis	Carbon content	wt%	86.9	76.5
	Hydrogen content	wt%	10.7	11.7
	Oxygen content	wt%	< 0.5	11.1
	Nitrogen content	wt-ppm	2,000	55
	Sulfur content	wt-ppm	23,000	2
Carbon residue		wt%	10.9	0.27
Type analysis	Saturated	wt%	21.7	-
	Aromatics	wt%	58.7	-
	Resin	wt%	10.8	-
	Asphaltene	wt%	8.8	-
Fatty acids	Palmitic (C16:0)	vol.%	-	13.8
	Palmitoleic (C16:1)	vol.%	-	0.8
	Margaric (17:0)	vol%	-	0.1
	Stearic (C18:0)	vol.%	-	6.8
	Oleic (C18:1)	vol.%	-	44.5
	Linoleic (C18:2)	vol.%	-	33.6
	Linolenic (C18:3)	vol.%	-	0.2
	Arachic (C20:0)	vol.%	-	0.2

viscosity is lower than that of C-heavy oil. This indicates that employing CJO can reduce heating energy required for atomization of the fuel. The flash point of CJO is much higher than that of C-heavy oil, but the ignition points of both fuels are almost identical. It should be noted that CJO contains more than 10 wt.% oxygen in its molecular composition. The oxygen content of the fuel molecules has been found to affect the sooting tendency [40]. The nitrogen and sulfur contents and the carbon residue of CJO are considerably lower than that of C-heavy oil. Hence, the NOx, SOx and particulate matter emissions from CJO combustion are expected to be lower than that from C-heavy oil combustion.

2.2 Liquid fuel combustion test furnace

Figure 1 is a schematic diagram of the liquid fuel combustion test facility at the Central Research Institute of Electric Power Industry (CRIEPI). This facility was designed to evaluate the liquid fuel

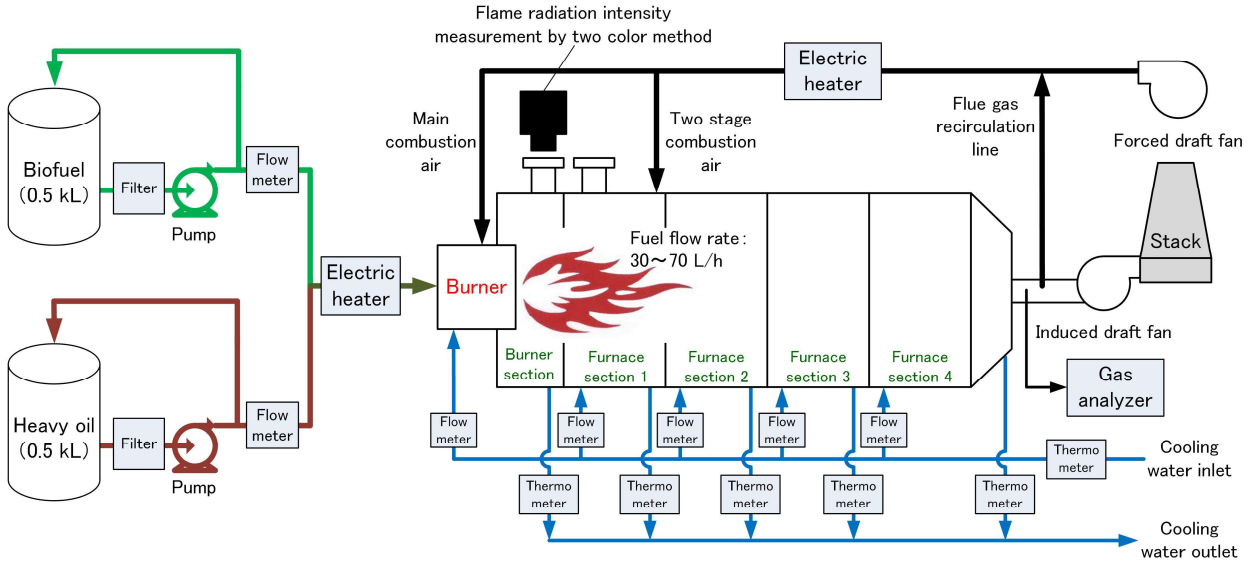

Fig. 1. Schematic of liquid fuel combustion test facility.

59 combustion characteristics of oil-fired thermal power stations. Two types of fuels in arbitrary mixing
60 ratios could be supplied to the furnace. The steam heater heated the tanks and fuel lines. The fuel
61 temperature supplied to the burner nozzle could be controlled up to 150 ºC by the electric heater in
62 front of the fuel nozzle. The furnace was divided into five sections to measure the heat absorption
63 balance using the inlet and outlet temperatures of the cooling water and the flow rates of each section.
64 The detailed procedure to measure the heat absorption balance was as follows. Cooling water at room
65 temperature (20-30 ºC) was supplied to each section during the combustion experiment. The flow rate
66 of the cooling water to each section was adjusted to be sufficiently large to avoid boiling the cooling
67 water. As indicated in Fig. 1, the temperature and the flow rate of the cooling water to each section
68 were measured by a thermometer and flowmeters. The temperatures of the return cooling water from
69 each section (40-60 ºC) were also measured by thermometers. The heat absorption rate of each section
70 was then calculated using the following formula:
71
72 $$\dot{Q}_i = \dot{m}_{water,i} c_{p,water} \left(T_{out,i} - T_{in} \right). \quad (1)$$

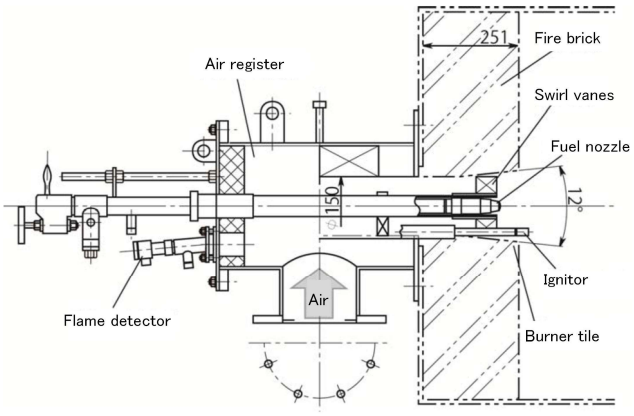

Fig. 2. Details of burner.

73

74 Here, Q_i, $m_{water,i}$, $T_{out,i}$, and T_{in} are the heat absorption rate of section i [W], the mass flowrate of cooling
75 water supplied to section i [kg/s], the temperature of cooling water discharged from section i [K], and
76 the temperature of cooling water supplied to each section [K], respectively. The combustion air was
77 supplied from a forced draft fan. Mixing the exhaust gas with the air supply line allowed the
78 recirculation of a portion of the exhaust gas. The air temperature could be heated up to 280 ºC by the
79 electric heaters.

80 Figure 2 shows the details of the burner (Volcano Co., Ltd) that was designed to combust C-heavy oil.
81 The burner contained swirl vanes for stabilizing the flames. An electric discharge from a spark igniter
82 resulted in ignition. A flame detector was installed to monitor the extinction of the flames during the
83 experiment.

84 Figure 3 shows the details of the fuel-atomizing nozzle. A steam atomizer with a mixing chamber was
85 employed as the fuel-atomizing nozzle. The supplied steam pressure was controlled at a constant value
86 during the experiment.

87

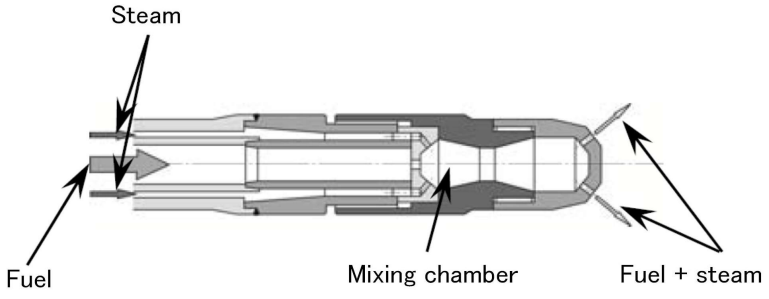

Fig. 3. Details of fuel atomizing nozzle.

88 **2.3 Measurement instruments and methods**

89 A two-color pyrometer (Thermera-Turret, Mitsui Optics Co., Ltd.) was used to measure the flame
90 radiation intensity through the optical window of the furnace as indicated in Fig. 1. The flame radiation
91 intensity was calculated from the *KL* value and the temperature which were measured by the two-color
92 method. The two-color method for the *KL* value and the temperature was based on the work of Hottel
93 and Broughton [41]. The thermal radiation intensity from the soot particles was expressed by Planck's
94 equation with Wien's approximation law as follows:

95

96 $$E_{\lambda i} = \frac{C_1 \varepsilon_{\lambda i}}{\lambda_i^5} \exp\left[-\frac{C_2}{\lambda_i T} \right] \quad (2)$$

97

98 Here, $\varepsilon_{\lambda i}$ is expressed by the following empirical equation [41]:

99

100 $$\varepsilon_{\lambda i} = 1 - \exp\left[-\frac{KL}{\lambda_i^{\alpha}} \right] \quad (3)$$

101

102 In this study, the value of 1.38 was employed for α, as proposed by Matsui et al. [42]. Eq. (3) and the
103 measured thermal radiation intensities for two different wavelengths were substituted into Eq. (2), to
104 obtain the following equation:

105

$$\left[1-\frac{\lambda_1^5 E_{\lambda 1}\left(\exp\left[C_2/\lambda_1 T\right]-1\right)}{C_1}\right]^{\lambda_1^\alpha}-\left[1-\frac{\lambda_2^5 E_{\lambda 2}\left(\exp\left[C_2/\lambda_2 T\right]-1\right)}{C_1}\right]^{\lambda_2^\alpha}=0 \quad (4)$$

In this study, to avoid the superposition of the radical emission and chemiluminescence on the thermal radiation, 550 and 650 nm were employed for λ_1 and λ_2, respectively. The temperature, T, was calculated from Eq. (4). The value of KL was calculated from Eqs. (2) and (3) using previously calculated T. The flame radiation intensity E was calculated by integrating E_λ with respect to λ as follows:

$$E=\int_0^\infty E_\lambda d\lambda=\int_0^\infty\left(\frac{C_1\left(1-\exp\left[-KL/\lambda^\alpha\right]\right)}{\lambda^5}\exp\left[-\frac{C_2}{\lambda T}\right]\right)d\lambda \quad (5)$$

The maximum uncertainty for the measurement value of E_λ is 3%.

A gas analyzer measured the concentrations of CO, NOx, and SO_2 in the furnace exhaust gas. The maximum uncertainty for the measurements of CO, NOx, and SO_2 was 5 ppm. In the current research, NOx, CO, and SO_2 emissions were evaluated as their volumetric concentration in the exhaust gas was corrected to 4% O_2. The corrected concentration was calculated by Eq. (6):

$$X_{4\%O2,i}=X_{measured,i}\frac{\left(20.99-4\right)}{\left(20.99-X_{m,O2}\right)} \quad (6)$$

Here, $X_{4\%O2,i}$, $X_{measured,i}$, and $X_{m,O2}$ were the concentrations corrected to 4% O_2 of species i [ppm], the measured concentration of species i in the exhaust gas [ppm], and the measured concentration of O_2 in the exhaust gas [%], respectively.

The concentrations and size distributions of the particles in the exhaust gas were measured based on the Japanese Industrial Standards JIS-Z8808 [43], which prescribes the method for measuring dust concentrations of an exhaust gas in a flue, stack or duct, and JIS-K0302 [44], which prescribes the method for measuring particle size distribution of dusts in flue gas, respectively. In addition, a scanning electron microscope (SEM) was used to analyze the collected particles in detail.

2.4 Experimental conditions

Table 2 shows the experimental conditions in this research. In Case 1, 100% C-heavy oil was used as a fuel. A mixed fuel containing 50% CJO and 50% C-heavy oil on an LHV basis was used in Case 2. The fuel mass flow rates of CJO and C-heavy oil were controlled by small size rotary flow meters (Type R, Nitto Seiko co. ltd). In order to accurately control the mass-based fuel flow rate considering

Table 2 Experimental conditions.

	Case 1 (100% C-heavy oil)	Case 2 (50% CJO/50% C-heavy)
Thermal input [kW]	550	
Staged combustion air ratio [%]	15	
Exhaust gas recirculation ratio [%]	15	
Excess air ratio [-] (Oxygen mole fraction at exit [%])	1.26 (4.5)	
CJO flow rate [kg/h]	0	27
C-heavy oil flow rate [kg/h]	47	24
Air flow rate [Nm^3/h]	624	648
Fuel viscosity at nozzle [mm^2/s]	6.5	
Fuel temperature at nozzle [℃]	140	124
Atomization steam flow rate [kg/h]	0.01	

the liquid fuel density based on Table2, the temperatures of the flow meters were controlled at 50 ºC. The maximum uncertainty for the flow meters is 1.5% for full scale (200 L/h). Therefore, the maximum uncertainty for the flow meters was 5.1 – 5.7% for actual fuel flow rates (52.4 – 58.4 L/h). The fuel mass flow rate of CJO was higher than that of C-heavy oil in Case 2 because of the lower LHV of CJO. Both cases used the same values for the thermal input, the staged combustion air ratio, the exhaust gas recirculation ratio, the excess air ratio, the fuel viscosity at the nozzle and the atomization steam flow rate. The values of the staged combustion air ratio (15%) and the exhaust gas recirculation ratio (15%) were based on the common operating conditions across heavy oil-fired thermal power stations in Japan. As the spray characteristics of liquid fuel exert a strong effect on the combustion characteristics [45-47], the liquid fuel temperature was controlled such that there was no difference in liquid fuel viscosity between the two cases.

3 Results and discussion

3.1 Flame radiation intensity and heat absorption balance

Figure 4 shows a comparison of the direct photographs of the flames in Case 1 and Case 2. The same exposure time was used for both cases. Evidently, the flame luminosity in Case 1 is higher than that in Case 2. This indicates that the soot volume fraction of the flame in Case 2 is lower than that in Case 1. This tendency is consistent with that of the measured flame radiation intensity, as shown in Fig. 5.

Figure 5 shows the flame radiation intensity obtained by the two-color method described in detail in

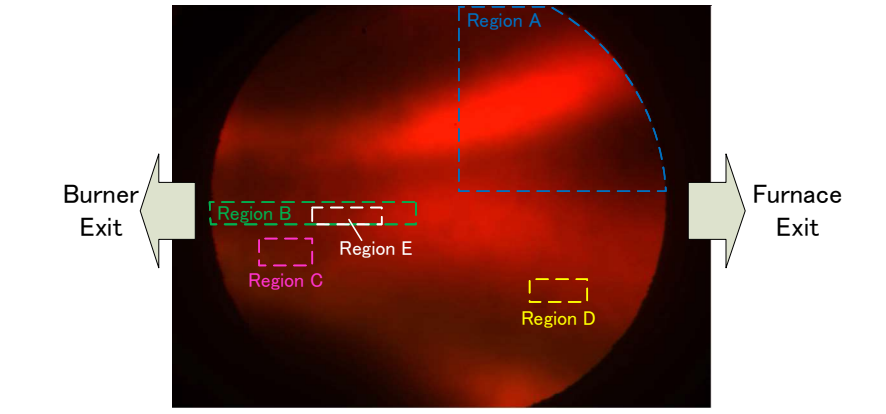

(a) Definition of each region

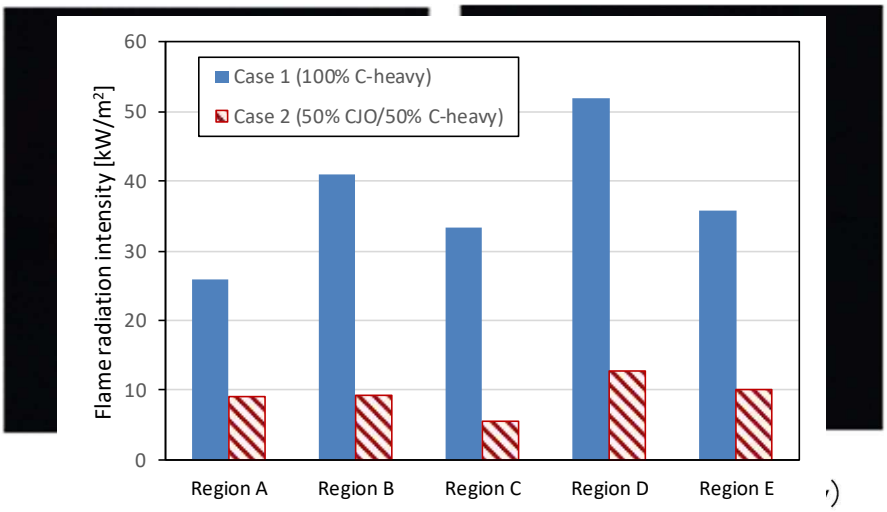

(b) Flame radiation intensity for each region

Fig. 5. Flame radiation intensity.

Fig. 4. Direct images of the flame (the same exposure time was used in both cases).

157 section 3.2. The measurement was conducted through the optical window nearest to the burner exit.
158 The location and size of each measurement region is indicated in Fig. 5 (a). Although there are some
159 differences in the absolute values between the regions, it is obvious that the flame radiation intensity
160 in Case 2 is lower than that in Case 1. This could be because CJO has no aromatic ring in its molecules.
161 The sooting tendency of the biofuel is lower than that of fossil fuel. In a previous study on the
162 combustion of pure Jatropha oil in gas turbine combustors, although the combustion conditions were
163 different, the same trend was observed [25]. The same tendency was also observed for the combustion
164 of other biofuels [48, 49]. Wang et al. [50] and Cignoli et al. [51] reported that the sooting tendency
165 of a fuel containing aromatic rings in its molecular composition was higher than that of a fuel
166 containing no aromatic rings. Additionally, Song et al. [40] found that the soot from a biofuel had a
167 high reactivity during combustion because of the presence of oxygen in the biofuel molecules. Figures
168 4 and 5 and the previous results cited above indicate that the mixing of a biofuel with a fossil fuel has
169 the effect of reducing the flame radiation intensity. This reduction in the flame radiation intensity might
170 affect the heat absorption balance of the furnace.

171 Figure 6 shows the heat absorption balances in Cases 1 and 2. The heat absorption ratios of the burner
172 section and the furnace section 1 (the nearest furnace section to the burner, as indicated in Fig. 1) in
173 Case 2 are lower than that in Case 1. This is caused by the lower flame radiation intensity in Case 2
174 due to the mixing of CJO, as observed in Fig. 5. The difference in the heat absorption balance between
175 two cases in this study is relatively small. Nevertheless, it is considered that the actual difference in
176 large scale boilers will exceed that in this study, because the proportion of the heat absorption quantity
177 due to thermal radiation to the heat absorption quantity due to thermal convection in large-scale boilers
178 is larger than that in small test furnaces [52]. In other words, due to the lower specific surface area of
179 the water wall, the radiation heat transfer plays a more important role in large scale boilers compared
180 with small furnaces. Because the flame radiation intensity has a strong correlation with the fuel spray
181 droplet diameter [25], the flame radiation intensity might be increased by increasing fuel spray fuel
182 droplet size. However, an increase in the fuel droplet size beyond a certain point could cause other
183 problems, such as flame extinction or an increase in the particulate matter concentration in the exhaust

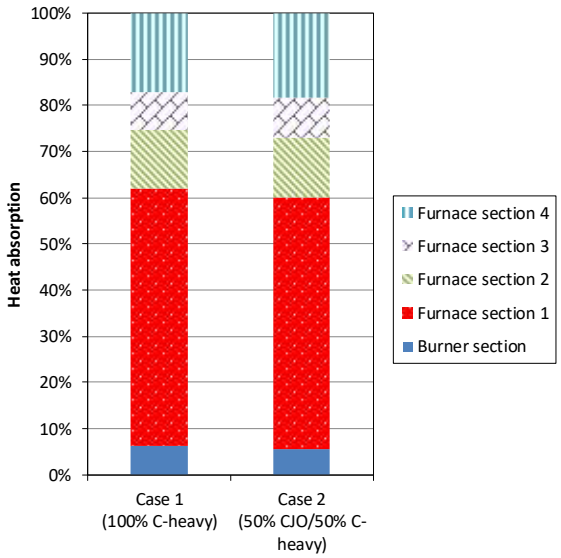

Fig. 6. Heat absorption balance of burner and furnace sections.

184 gas. Thus, there are limitations to increasing the fuel droplet size. Therefore, when CJO is introduced
185 at a high blending ratio into large-scale boilers, careful attention should be paid to the heat absorption
186 balance for operational safety.
187
188 **3.2 Emissions**
189 In both Cases 1 and 2, the concentration of CO in the exhaust gas was less than 10 ppm, and there
190 were no significant differences between the two cases.
191 Figure 7 shows the NOx emissions in Cases 1 and 2. The NOx emissions in Case 2 are lower than
192 those in Case 1. This is attributed to the lower nitrogen content of CJO compared with C-heavy oil.
193 The NOx is formed by both the thermal NOx mechanism and the fuel NOx mechanism in the spray
194 combustion field. Due to the inclusion of CJO with its lower nitrogen content, the amount of NOx
195 formed by the fuel NOx mechanism was decreased in Case 2. As the nitrogen content of CJO (55 wt.
196 ppm) is significantly lower than that of C-heavy oil (2000 wt. ppm), the nitrogen content of the mixed
197 fuel in Case 2 is almost half of that in Case 1. In spite of the fact mentioned above, the NOx emission
198 in Case 2 was not reduced by half compared with that in Case 1 (the NOx emission in Case 2 was
199 approximately 62% of that in Case 1). This is because a portion of the NOx is formed by the thermal
200 NOx mechanism. The amount of NOx formed by the thermal NOx mechanism is not significantly
201 affected by the fuel type, because the flame temperature does not significantly change for the fuel type
202 under the same excess air ratio. Therefore, the decrease in NOx emission in Case 2 is caused by the
203 reduction of NOx formed by the fuel NOx mechanism.

Figure 8 shows the SO_2 emissions in Case 1 and Case 2. The SO_2 emission in Case 2 is lower than that in Case 1. This is caused by the lower sulfur content of CJO compared to that of C-heavy oil. In contrast to the NOx emissions (Fig. 7), the SO_2 emission in Case 2 was approximately half that of Case 1 (the SO_2 emission in Case 2 was approximately 53% of that in Case 1). It has been established that all the sulfur present in fuel appears as SO_2 or SO_3 in the combustion products (the amount of SO_3 produced is typically only a few percent of the amount of SO_2) [53]. Hence, the SO_2 emission in Case 2 was reduced solely by the decrease in the sulfur content of the mixed fuel compared to 100% C-heavy oil. Slight difference between the measured value for Case 2 (53% of Case 1) and the expected value (50% of Case 2) is considered to be due to the uncertainty of flow meter of fuels (5.1 – 5.7%).

Figure 9 shows the particulate matter concentration in the exhaust gas. The particulate matter concentration in Case 2 is lower than that in Case 1. This is because, as indicated in Table 2, the carbon

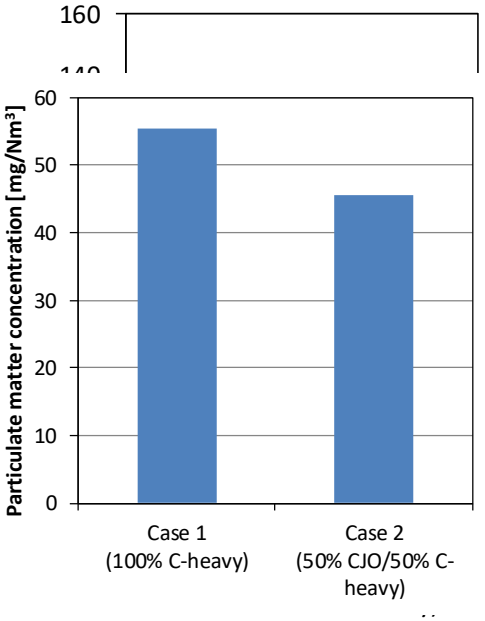

Fig. 9. Particulate matter emission.

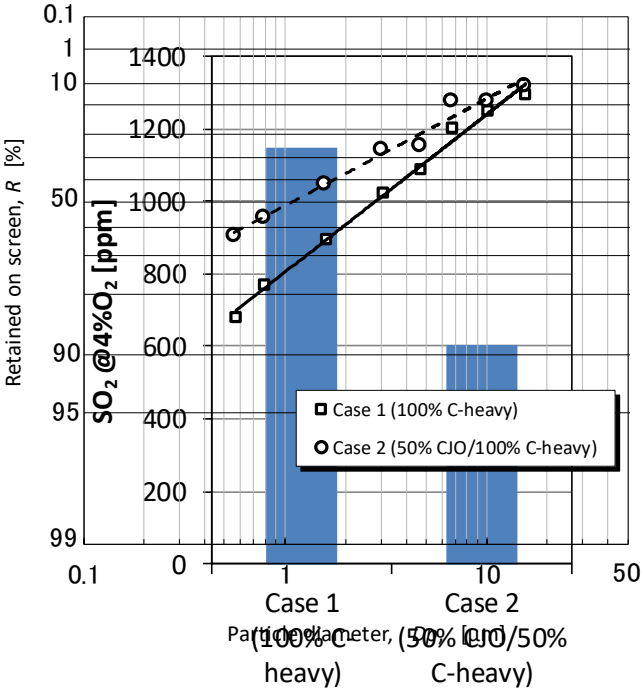

Fig. 10. Rosin-Rammlar plots for particles

Fig. 7. NOx emission.

Fig. 8. SO_2 emission.

residue of CJO is significantly lower than that of C-heavy oil. Generally, when the carbon residue in the liquid fuel is high, the particulate matter concentration in the exhaust gas tends to be high [54,55]. Figures 10 and 11 show Rosin-Rammlar plots for the particles collected from the exhaust gas and the SEM images of the particles. The particle sizes in Case 2 is entirely smaller than that in Case 1. This is because of the higher porosity of the particles in Case 2 compared with that in Case 1, as discussed below. Two types of particulate matter are emitted from liquid fuel combustion fields, namely, soot and cenospheres [56,57]. Soot is formed by the incomplete combustion of hydrocarbons in the gas phase due to a local lack of oxygen. Cenospheres are formed from the remaining heavy aromatic constituents of the fuel following thermal decomposition of the fuel. In general, the shapes and sizes of the soot particles and cenospheres from liquid fuel combustion fields are significantly different [58]. It is evident from the SEM images in Fig. 11 that most of the particulate matter collected from the exhaust gas consist of cenospheres, i.e., almost no soot particles can be observed in Fig. 11. There are also no significant differences in the basic sizes of the large cenospheres between the two cases (Fig. 11 (a) and (b)). This is because there are no significant differences in the spray characteristics between the two cases, as the fuel viscosities at the atomizing nozzle for the two cases are consistent. Thus, there was no significant difference in the size distribution of droplets injected from the fuel nozzle to the combustion field between the two cases. However, the number and sizes of the open holes on the cenosphere surface in Case 2 (Fig. 11 (d)) are greater than that in Case 1 (Fig. 11 (c)). This is because the carbon residue content of CJO is significantly lower than that of C-heavy oil. The concentration of heavy aromatic constituents of the fuel in Case 2 was diluted by the mixing with CJO. Hence, the

235 proportion of volatile matter in the fuel droplets in Case 2 is larger than that in Case 1. Consequently,
236 the porosity of the cenospheres in Case 2 was higher than that in Case 1. Many collapsed cenospheres
237 are observed in Case 2 (Fig. 11 (b)), while there are fewer collapsed cenospheres in Case 1 (Fig. 11
238 (a)). The particle sizes of the collapsed cenospheres are smaller than that of the original cenospheres.
239 This is considered to explain why the particle sizes in Case 2 are consistently smaller than that in Case
240 1, as observed in Fig. 10.
241 As per the above discussion, this study verified that the emissions of NOx, SO_2 and particulate matter
242 from the furnace could be decreased by the mixing of CJO with C-heavy oil. However, it should be

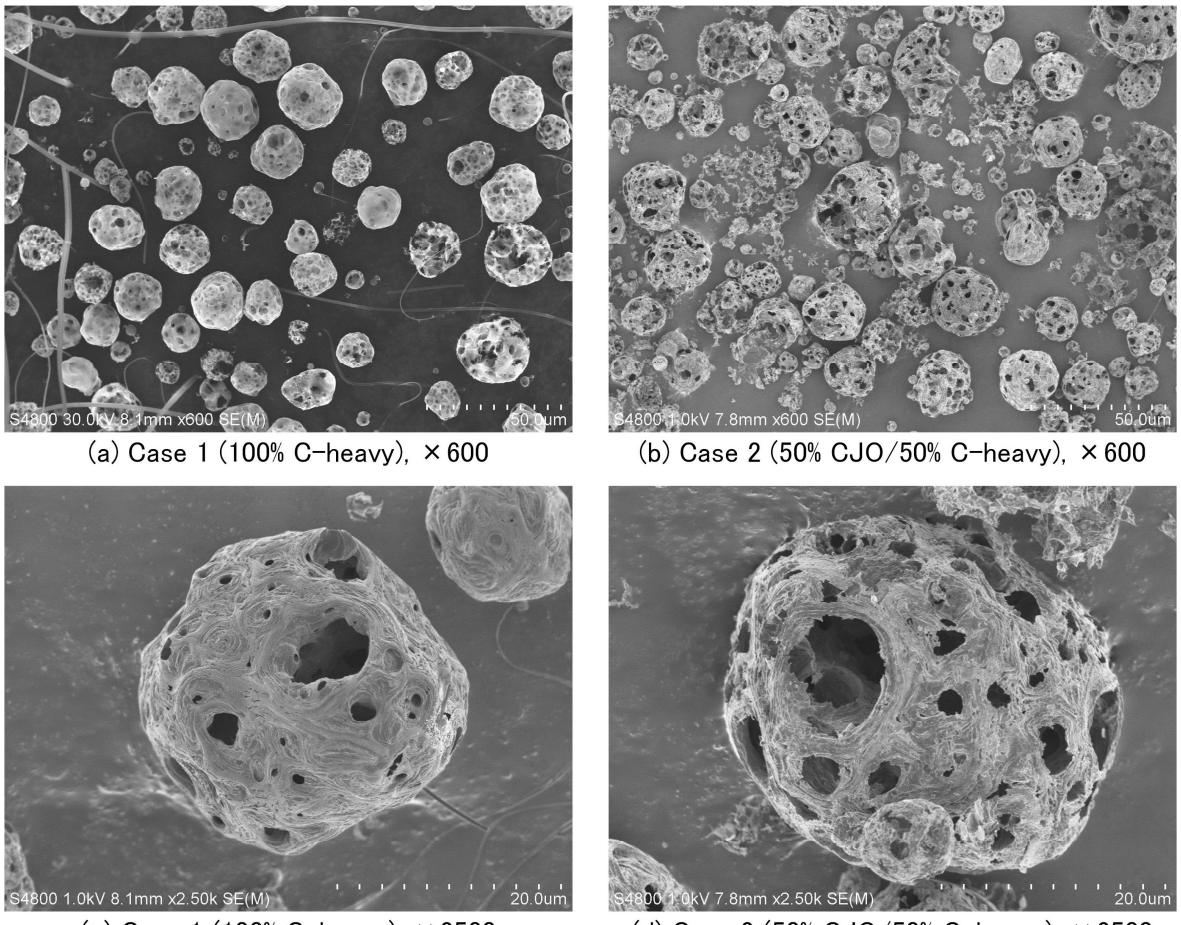

(a) Case 1 (100% C-heavy), ×600
(b) Case 2 (50% CJO/50% C-heavy), ×600
(c) Case 1 (100% C-heavy), ×2500
(d) Case 2 (50% CJO/50% C-heavy), ×2500

Fig. 11. SEM images of particles collected from exhaust gas.

noted there is a possibility of decreasing the particle collection efficiency of the electrostatic precipitator (ESP). This is because a penetration window from a few percent up to tens of percent exists in the size range from 0.1 to 5 μm for a normally operating ESP [59]. Therefore, careful attention to the particle size distributions in the exhaust gas is required when introducing CJO into oil-fired thermal power stations.

4. Conclusions

This study investigated the effect of crude *Jatropha* oil (CJO) blended with C-heavy oil on the combustion characteristics of oil-fired boilers. The combustion experiments were conducted using a 550 kW liquid combustion test facility equipped with a steam atomizing burner. The flame radiation intensity, the heat absorption balance of the furnace and the emissions of NOx, SO_2, and the particulate matter in the 50%CJO + 50% C-heavy oil case were compared with that in the 100% C-heavy oil case. The size distributions of the particles collected from the exhaust gas were also analyzed. The principal findings are as follows.

1. The flame radiation intensity was decreased using CJO blended with C-heavy oil. This was considered to be due to the low sooting tendency of CJO. The low sooting tendency of CJO is due to that CJO has no aromatic ring in its molecules and it has higher oxygen content than C-heavy oil.
2. The heat absorption of the section near the burner was decreased using CJO blended with C-heavy

oil. This was caused by the decrease in the flame radiation intensity. The decrease in the flame radiation intensity is due to the low sooting flame tendency of CJO. As this effect is greater in actual large scale boilers, careful attention should be paid to the heat absorption balance when CJO is introduced into large scale boilers at a high blending ratio.

3. The NOx and SO_2 emissions were greatly decreased using CJO blended with C-heavy oil. This was because the nitrogen and sulfur contents of CJO were significantly lower than that of C-heavy oil. The SO_2 emission in the 50% CJO + 50% C-heavy oil case was approximately half that of the 100% C-heavy oil case. However, the NOx emission in the 50% CJO + 50% C-heavy oil case was more than 60% of that in the 100% C-heavy oil case. This was because a portion of the NOx was formed by the thermal NOx mechanism, and the nitrogen content of fuel did not affect this mechanism.

4. Both the particulate matter emission and the size of the particulate matter were decreased using CJO blended with C-heavy oil. This was due to the lower carbon residue in CJO compared to C-heavy oil. The decrease in the particle size was caused by the fact that the cenospheres in the CJO blending case were broken into small particles because of their high porosity. Hence, careful attention should be paid to the possibility of a decrease in the particle collection efficiency of the electrostatic precipitator due to the decrease in particle size when CJO is introduced into oil-fired thermal power stations.

References

[1] Jongschaap, R. E. E., W. J. Corré, P. S. Bindraban, and W. A. Brandenburg, 2007. Claims and Facts on Jatropha curcas L. Plant Research International B.V., Wageningen, the Netherlands, Report 158, 42 pp + annexes.

[2] GEXSI, Global Market Study on Jatropha: Final Report, 2008.

[3] May CY, Hgan MA, Weng CK, Basiron Y. Palm diesel: An option for greenhouse gas mitigation in the energy sector. Journal of Oil Palm Research 2005;17:47-52.

[4] Pandey KK, Pragya N, Sahoo PK. Life cycle assessment of small-scale high-input Jatropha biodiesel production in India. Applied Energy 2011;88:4831-9.

[5] Rahim NA, Jaafar MNM, Sapee S, Elraheem HF. Effect on particulate and gas emissions by combusting biodiesel blend fuels made from different plant oil feedstocks in a liquid fuel burner. Enegies 2016;9:659.

[6] Desmira N, Kitagawa K, Morita S, Gupta AK. In-situ spectroscopic monitoring of Jatropha oil combustion properties. Renewable Energy 2014;63:775-8.

[7] Murali Krishna MVS, Ohm Prakash T, Ushasri P, Janardhan N, Murthy PVK. Experimental investigations on direct injection diesel engine with ceramic coated combustion chamber with carbureted alcohols and crude jatropha oil. Renewable Sustainable Energy Rev 2016;53:606-28.

[8] Tsuchiya Y, Okajima I, Sako T. Study on the performance and emissions of diesel engines fueled by jatropha crude oil extracted with supercritical CO_2. J Chem Eng Japan 2016;49:217-23.

[9] Mangus M, Kiani F, Mattson J, Tabakh E, Petka J, Depcik C, Peltier E, Stagg-Williams S. Investigating the compression ignition combustion of multiple biodiesel/ULSD (ultra-low sulfur diesel) blends via common-rail injection. Energy 2015;89:932-45.

[10] Puhan S, Saravanan N, Nagarajan G, Vedaraman N, Effect of biodiesel unsaturated fatty acid on combustion characteristics of a DI compression ignition engine. Biomass Bioenergy 2010;34:1079-88.

[11] Banapurmath NR, Marikatti MK, Hunashyat AM, Tewari PG. Combustion characteristics of a four-stroke CI engine operated on Honge and Jatropha oil methyl ester–ethanol blends when directly injected and dual fuelled with CNG induction. Int J Sustainable Engineering 2011;4:142-52.

[12] Banapurmath NR, Tewari PG, Hosmath RS. Performance and emission characteristics of a DI compression ignition engine operated on Honge, Jatropha and sesame oil methyl esters. Renewable Energy 2008;33:1982-8.

[13] Chauhan BS, Kumar N, Cho HM, Lim HC. A study on the performance and emission of a diesel engine fueled with Karanja biodiesel and its blends. Energy 2013;56:1-7.

[14] de Azevedo CG, de Andrade JC, de Souza Costa F. Effects of injector tip design on the spray characteristics of soy methyl ester biodiesel in a blurry injector. Renewable Energy 2016;85:287-94.

[15] Dubey P, Gupta R. Influences of dual bio-fuel (Jatropha biodiesel and turpentine oil) on single cylinder variable compression ratio diesel engine. Renewable Energy 2018;115:1294-302.

[16] Jain S, Sharma MP. Engine performance and emission analysis using oxidatively stabilized Jatropha curcas biodiesel. Fuel 2013;106:152-6.

[17] Kannan D, Pachamuthu S, Nabi Md.N, Hustad JE, Løvås T. Theoretical and experimental

investigation of diesel engine performance, combustion and emissions analysis fuelled with the blends of ethanol, diesel and jatropha methyl ester. Energy Coversion Management 2012;53:322-31.
[18] Westphal GA, Krahl J, Munack A, Rosenkranz N, Schröder O, Schaak J, Pabst C, Brüning T, Bünger J. Combustion of hydrotreated vegetable oil and Jatropha methyl ester in a heavy duty engine: Emissions and bacterial mutagenicity. Environ Sci Tech 2013;47:6038-46.
[19] Nitiema-Yefanova S, Tschamber V, Richard R, Thiebaud-Roux S, Bouyssiere B, Bonzi-Coulibaly YL, Nebie RHC, Coniglio L. Ethyl biodiesels derived from non-edible oils within the biorefinery concept e Pilot scale production & engine emissions. Renewable Energy 2017;109:634-45.
[20] Hossain AK, Davies PA. Performance, emission and combustion characteristics of an indirect injection (IDI) multi-cylinder compression ignition (CI) engine operating on neat jatropha and karanj oils preheated by jacket water. Biomass Bioenergy 2012;46:332-42.
[21] Pradhan P, Raheman H, Padhee D. Combustion and performance of a diesel engine with preheated Jatropha curcas oil using waste heat from exhaust gas. Fuel 2014;115:527-33.
[22] Imtenan S, Masjuki HH, Varman M, Rizwanul Fattah IM, Sajjad H, Arbab MI. Effect of n-butanol and diethyl ether as oxygenated additives on combustion–emission-performance characteristics of a multiple cylinder diesel engine fuelled with diesel–jatropha biodiesel blend. Energy Conversion Management 2015;94:84-94.
[23] Patel C, Lee S, Tiwari N, Agarwal AK, Lee CS, Park S. Spray characterization, combustion, noise and vibrations investigations of Jatropha biodiesel fuelled genset engine. Fuel 2016;185:410-20.
[24] Nguyen KB, Dan T, Asano I. Effect of double injection on combustion, performance and emissions of Jatropha water emulsion fueled direct-injection diesel engine. Energy 2015;80:746-55.
[25] Hashimoto N, Nishida H, Ozawa Y. Fundamental combustion characteristics of Jatropha oil as alternative fuel for gas turbines. Fuel 126;2014:194-201.
[26] Badami M, Nuccio P, Pastrone D, Signoretto A. Performance of a small-scale turbojet engine fed with traditional and alternative fuels. Energy Conversion Management 2014;82:219-28.
[27] Rehman A, Phalke DR, Pandey R. Alternative fuel for gas turbine: Esterified jatropha oil-diesel blend. Renewable Energy 2011;36:2635-40.
[28] Fan Y, Hashimoto N, Nishida H, Ozawa Y. Spray characterization of an air-assist pressure-swirl atomizer injecting high-viscosity Jatropha oils. Fuel 2014;121:271-283.
[29] Chong CT, Hochgreb S. Flame structure, spectroscopy and emissions quantification of rapeseed biodiesel under model gas turbine conditions. Applied Energy 2017;185:1383-92.
[30] Somorin TO, Kolios AJ. Prospects of deployment of Jatropha biodiesel-fired plants in Nigeria's power sector. Energy 2017;135:726-39.
[31] Sivakumar D, Vankeswaram SK, Sakthikumar R, Raghunandan BN, Hub JTC, Sinha AK. Fuel 2016;179:36-44.
[32] Kang SB, Kim JJ, Im YH. An experimental investigation of a direct burning of crude Jatropha oil (CJO) and pitch in a commercial boiler system. Renewable Energy 2013;54:8-12.
[33] Mikami M, Kikuchi M, Kan Y, Seo T, Nomura H, Suganuma Y, Moriue O, Dietrich DL. Droplet cloud combustion experiment "Group combustion" in KIBO on ISS. Int J Microgravity Sci Appl 2016;33:330208.

[34] Sano N, Motomatsu N, Saputro H, Seo T, Mikami M. Flame-spread characteristics of n-Decane droplet arrays at different ambient pressures in microgravity. Int J Microgravity Sci Appl 2016;33:330108.
[35] Nakaya S, Fujishima K, Tsue M, Kono M, Segawa D. Effects of droplet diameter on instantaneous burning rate of isolated fuel droplets in argon-rich or carbon dioxide-rich ambiences under microgravity. Proc Combust Inst 2013;34:1601-8.
[36] Nomura H, Takahashi H, Suganuma Y, Kikuchi M. Droplet ignition behavior in the vicinity of the leading edge of a flame spreading along a fuel droplet array in fuel-vapor/air mixture. Proc Combust Inst 2013;34:1593-600.
[37] Hashimoto N, Nomura H, Suzuki M, Matsumoto T, Nishida H, Ozawa Y. Evaporation characteristics of a palm methyl ester droplet under a high ambient temperature. Fuel 2015;143:202-10.
[38] Atzler F, Demoulin FX, Lawes M, Lee Y, Marquez N. (2006) Burning rates and flame oscillations in globally homogeneous two-phase mixtures (Flame speed oscillations in droplet cloud flames). Combust Sci Tech 2006;178:2177-98.
[39] Nishida H, Hashimoto N, Kimoto M. Applicability assessments of liquid fuels for thermal power generation plants – 1st report: Evaluation of the combustion characteristics at the renewed coal and liquid fuel combustion test furnace, Tokyo, CRIEPI Report M14003, 2015 (in Japanese).
[40] Song J, Alam M, Boehman AL, Kim U. Examination of the oxidation behavior of biodiesel soot. Combust Flame 2006;146:589–604.
[41] Hottel HC, Broughton FP. Determination of true temperature and total radiation from luminous gas flames: Use of special two-color optical pyrometer. Ind. Eng. Chem. Anal. Ed. 1932;4:166-75.
[42] Matsui Y, Kamimoto T, Matsuoka S. A study on the time and space resolved measurement of flame temperature and soot concentration in a D. I. diesel engine by the two-color method. SAE technical paper 790491; 1979.
[43] JIS Z 8808: 2013. Methods of measuring dust concentration in flue gas.
[44] JIS K 0302: 1989. Measuring method for particle-size distribution of dusts in flue gas.
[45] Chong CT, Hochgreb S. Spray flame structure of rapeseed biodiesel and Jet-A1 fuel. Fuel 2014;115:551-8.
[46] Chong CT, Hochgreb S. Spray and combustion characteristics of biodiesel: Non-reacting and reacting. Int Biodeterioration & Biodegradation. 2015;102:353-60.
[47] Hayashi J, Watanabe H, Kurose R, Akamatsu F. Effect of fuel droplet size on soot formation in spray flames formed in a laminar counterflow. Combust Flame 2011;158:2559-68.
[48] Allouis C, Romano M, Beretta F, Viegas L, D'Alessio A. Particulate formation from the spray combustion of heavy oil and biofuel. Combust Sci Tech 1998;134:457-75.
[49] Hashimoto N, Ozawa Y, Mori N, Yuri I, Hisamatsu T. Fundamental combustion characteristics of palm methyl ester (PME) as alternative fuel for gas turbines. Fuel 2008;87:3373-8.
[50] Wang R, Cadman P. Soot and PAH production from spray combustion of different hydrocarbons behind reflected shock waves. Combust Flame 1998;112:359–70.
[51] Cignoli F, De Iuliis S, Zizak G. Soot load versus aromatic concentration in diesel oil premixed

flames. Fuel 2001;80:945–55.
[52] Hashimoto N, Watanabe H. Numerical analysis on effect of furnace scale on heat transfer mechanism of coal particles in pulverized coal combustion field. Fuel Processing Tech 2016;145:20-30.
[53] Turns SR. An introduction to combustion: Concepts and applications. 3rd ed. New York: McGraw-Hill; 2012.
[54] Asai T, Koizumi H, Yoshida S, Inoue H. Effects of fuel-nozzle configurations on particulate-matter emissions from a model gas turbine combustor. Proc ASME Turbo Expo 2008, GT2008-50351, pp. 229-38, 2008.
[55] Ichinose T, Fujimura K, Takeno K, Motai T, Arakawa Y, Fujii H. Combustion characteristics and pollution minimum technology for VR (Vacuum Residue) fired boiler. JSME Int J Series B: Fluids and Thermal Engineering 1998;41:1055-60.
[56] Williams A. Fundamentals of oil combustion. Prog Energy Combust Sci 1976;2:167-179.
[57] Moszkowicz P, Witzel L, Claus G. Modelling of very fast pyrolysis of heavy fuel oil droplets. Chem Eng Sci 1996;51:4075-86.
[58] Bartle KD, Jones JM, Lea-Langton AR, Pourkashanian M, Ross AB, Thillaimuthu JS, Waller PR, Williams A. The combustion of droplets of high-asphaltene heavy oils. Fuel 2013;103:835-42.
[59] Ylätalo SI, Hautanen J. Electrostatic precipitator penetration function for pulverized coal combustion. Aerosol Sci Tech 1998;29:17-30.

Figure and table captions